RENAL FAILURE
2025, VOL. 47, NO. 1, 2559093
https://doi.org/10.1080/0886022X.2025.2559093

Taylor & Francis
Taylor & Francis Group

LABORATORY STUDY

Significance of neutrophil extracellular traps and low-density granulocytes in advanced chronic kidney disease (stage 5D) cases with COVID-19

Wiwat Chancharoenthana[a,b,c], Supitcha Kamolratanakul[a,b], Wassawon Ariyanon[d], Thansita Bhunyakarnjanarat[e,f], Hailong Hu[g,h], Opas Traitanon[c,i], Asada Leelahavanichkul[e,f], Marcus J. Schultz[j,k,l] and Claudio Ronco[m,n,o]

[a]Department of Clinical Tropical Medicine, Faculty of Tropical Medicine, Mahidol University, Bangkok, Thailand; [b]Tropical Immunology and Translational Research Unit (TITRU), Department of Clinical Tropical Medicine, Faculty of Tropical Medicine, Mahidol University, Bangkok, Thailand; [c]Thammasat Multi-Organ Transplant Center, Thammasat University Hospital, Faculty of Medicine, Thammasat University, Pathum Thani, Thailand; [d]Department of Medicine, Banphaeo General Hospital (BGH), Samutsakhon, Thailand; [e]Immunology Unit, Department of Microbiology, Faculty of Medicine, Chulalongkorn University, Bangkok, Thailand; [f]Center of Excellence in Translational Research in Inflammation and Immunology (CETRII), Department of Microbiology, Faculty of Medicine, Chulalongkorn University, Bangkok, Thailand; [g]Center for Computational and Genomic Medicine, The Children's Hospital of Philadelphia, Philadelphia, PA, USA; [h]Department of Pathology and Laboratory Medicine, University of Pennsylvania, Philadelphia, PA, USA; [i]Division of Nephrology, Department of Medicine, Faculty of Medicine, Thammasat University, Pathum Thani, Thailand; [j]Department of Intensive Care & Laboratory of Experimental Intensive Care and Anesthesiology (L.E.I.C.A), Academic Medical Center, University of Amsterdam, Amsterdam, Netherlands; [k]Mahidol-Oxford Tropical Medicine Research Unit (MORU), Mahidol University, Bangkok, Thailand; [l]Centre for Tropical Medicine and Global Health, Nuffield Department of Medicine, Oxford University, Oxford, United Kingdom; [m]International Renal Research Institute of Vicenza (IRRIV), Vicenza, Italy; [n]Department of Nephrology, Dialysis and Transplantation, San Bortolo Hospital, Vicenza, Italy; [o]Department of Medicine (DIMED), Università Degli Studi di Padova, Padua, Italy

ABSTRACT

Coronavirus disease 2019 (COVID-19) affected billions of individuals globally, with symptoms ranging from isolated blood clotting to severe acute hypoxemic respiratory failure requiring intensive respiratory support ventilators. Those with advanced chronic kidney disease (CKD stage 5) were at high risk of severe disease faced a particularly heightened risk of severe illness. Inflammation and associated immune-thrombotic events in CKD stage 5 have attracted increasing attention, yet remain poorly understood. In this prospective cohort study, we examined and compared neutrophil extracellular traps (NETs) and low-density granulocytes (LDGs) in heathy controls ($n=15$), CKD stage 5 patients without COVID-19 ($n=15$), patients with COVID-19 ($n=15$), and CKD stage 5 patients with COVID-19 ($n=90$). Serum citrullinated histone H3 (CitH3) and related gene expression (*PAD4, ERK1, PKC*), NET complexes, platelet factor 4 (PF4), von Willebrand factor (vWF), RANTES, and specific cytokines were quantified. Proof-of-concept experiments were conducted to assess the role of lipopolysaccharide-LDG complexes in NETs detected in COVID-19 plasma. NETs complexes were significantly higher in COVID-19 cases, and more so in patients with CKD stage 5D, and those who died. Disease severity was directly correlated with NETs complex levels ($p=0.016$). CitH3 and gene expression levels were not correlated with advanced CKD stage, while levels of components that initiate NETs formation were higher in patients with COVID-19 and in CKD stage 5 patients. In conclusion, NET activation could partially explain the thrombotic manifestations in patients with COVID-19 and in CKD stage 5 patients.

KEY POINTS

- NETs contribute to microthrombi in CKD stage 5D patients with COVID-19 severe lung injury.
- Both NETs and LDGs are potential indicators of early severe lung injury and mortality in COVID-19 with CKD stage 5D.

ARTICLE HISTORY

Received 24 May 2025
Revised 11 August 2025
Accepted 28 August 2025

KEYWORDS

Chronic kidney disease; COVID-19; end stage renal disease; low-density granulocytes; neutrophil extracellular traps; ventilator

CONTACT Wiwat Chancharoenthana wiwat.cha@mahidol.ac.th Department of Clinical Tropical Medicine, Faculty of Tropical Medicine, Mahidol University 16/F Ratchanakarin Building 420/6 Rajvithi Rd., Ratchathewi, Bangkok 10400, Thailand; Asada Leelahavanichkul aleelahavanit@gmail.com Immunology Unit, Department of Microbiology, Chulalongkorn University, Bangkok 10330, Thailand.

Introduction

The family of severe acute respiratory syndrome (SARS) coronavirus (CoV) includes SARS-CoV-2, the causative agent of coronavirus disease 2019 (COVID-19), primarily characterized by pulmonary infiltration [1]. The COVID-19 outbreak has transitioned from a pandemic to an endemic state, infections continue to present challenges in certain clinical situations [2,3], necessitating deeper understanding of disease pathogenesis and the development of novel treatments.

Patients with preexisting medical conditions have higher mortality rates when infected with COVID-19 [4]; for example, patients with stage 5 chronic kidney disease (CKD) have been found to be highly susceptible to develop COVID-19 and to have worse overall prognosis than the general population [5]. Indeed, studies have shown that despite being presented with similar initial disease severity, patients with preexisting CKD who contract COVID-19 suffer from significantly higher rates of acute kidney injury and mortality, with risk escalating as CKD stage progresses [6]. Uremic toxins are detrimental to multiple organs in patients with CKD stage 5 [7], and SARS-CoV-2 virus can directly infect various organs, including the kidney [1]. Several parameters are common to both CKD stage 5 with dialysis dependence (CKD stage 5D) and COVID-19 infection, including elevated blood proinflammatory cytokine levels, impaired intestinal barrier function, circulating endotoxins, lung damage, and disrupted brain function [8–10]. This confluence of pathologies is particularly dangerous, as the systemic inflammation and cytokine surge characteristic of severe COVID-19 can precipitate a pro-thrombotic state, a risk that is amplified in patients with renal compromise, such as kidney transplant recipients [11].

Moreover, individuals afflicted with both CKD stage 5D and COVID-19 infection may experience alterations in various indicators, especially those with severe infection; both conditions elicit comparable inflammatory responses, including heightened innate immune system activation, particularly of neutrophil extracellular traps (NETs) and low-density granulocytes (LDGs) [12–18]. The role of NETs, in particular, has gained significant attention, with systematic reviews concluding that elevated NET levels are predictive of key clinical outcomes in COVID-19, including the need for mechanical ventilation, thrombosis, and mortality [19], making them a critical target of investigation in high-risk groups like the CKD population.

NETs are formed by release of extracellular DNA networks from polymorphonuclear leukocytes (PMNs; including neutrophils), in response to activators, including viruses, uremic toxin, reactive oxygen species, and cell-free DNA, primarily through the peptidylarginine deiminase 4 (PAD4)-induced citrullinated histone H3 (CitH3) pathway [12–14]. LDGs are neutrophils in the peripheral blood mononuclear cell (PBMC) fraction with lower density than regular neutrophils after gradient separation [15], and are associated with the severity of both COVID-19 infection[16] and uremia [17], similar to NETs [1,18]. NETs and LDGs have potential value for assessing individuals with both CKD stage 5D and COVID-19 infection; however, existing insights with both illnesses are limited. Furthermore, gradient separation for LDG measurement is a simple method, accessible for most laboratories in resource-limited settings, potentially facilitating its application as a biomarker.

We hypothesized that CKD stage 5D could disrupt certain elements of COVID-19, including NETs and LDGs. Here, we report evidence that increased NET formation correlates with COVID-19 and the severity of hypoxemic respiratory failure. NET may serve as a biomarker for disease severity in patients with CKD stage 5D and COVID-19 who develop respiratory failure. Additionally, we show that patients with COVID-19 and CKD stage 5D have elevated RANTES and plasma factor 4 (PF4) levels, both of which can induce NETosis [20].

Methods

Participants and study design

This was a prospective observational study performed in Bangkok, Thailand. The study was approved by the Ethics Committee of the Faculty of Tropical Medicine, Mahidol University (reference number, MUTM 2022-022-01). The study protocols adhered to the Declaration of Helsinki guidelines and the International Conference on Harmonization Good Clinical Practice. Written informed consent was obtained from participant or legal guardian for study participation. All patient samples were de-identified and re-labeled after collection to maintain patient privacy.

Adult (aged ≥18 years) patients with CKD stage 5D and a first COVID-19 infection, with symptoms starting within 4 days (<96 h) after exposure, were consecutively enrolled from April 1, 2022, to March 31, 2023. COVID-19 infection cases were stratified for severity, as mild (mild clinical symptoms without imaging features of pneumonia), moderate (clinical symptoms, such as fever and cough, with imaging features of pneumonia), or severe (dyspnea, respiratory rate >30/min, blood oxygen saturation <93%, partial pressure of arterial oxygen to fraction of inspired oxygen ratio <300, and/or lung infiltrates >50% within 24–48 h) [21,22]. CKD stage 5D was defined by estimated glomerular filtration rate (eGFR) using the Chronic Kidney Disease Epidemiology Collaboration (CKD-EPI) equation [23] of <15 mL/min/1.75 m^2 along with dialysis dependence. Exclusion criteria were COVID-19 patients with multiple organ dysfunction syndrome, coagulopathy, other previous infections within 4 weeks prior to COVID-19 infection, expected survival time <48 h, and other chronic conditions involving organ damage, including cirrhosis, cardiomyopathy, chronic obstructive lung disease, etc. Healthy controls ($n=15$) and patients with COVID-19 without CKD ($n=15$) served as controls. These subjects had eGFR >90 mL/min/1.75 m^2, whereas CKD stage 5D controls (non-COVID-19) ($n=15$) with stable health status and no history of prior COVID-19 infection were recruited from an online-hemodiafiltration hemodialysis unit (Figure 1). All recruited individuals provided written consent.

COVID-19 diagnosis was confirmed by quantitative analysis of SARS-CoV-2 E and N genes by polymerase chain reaction (PCR) using nasopharynx, nasal swab, or deep throat saliva samples, with a cycle threshold value <25 (all viral gene targets) within the previous 24 h (ensuring that recruited patients had high viral loads). Chest radiography and biochemical parameters were assessed at enrollment, including complete blood count, serum biochemical tests (liver and renal function, and electrolytes), coagulation profile, high sensitivity C-reactive protein, D-dimers, and procalcitonin. Comorbidity burden was quantified using the Charlson Comorbidity Index. Disease severity and organ dysfunction were recorded for all patients admitted to the intensive care unit (ICU) by monitoring basal clinical functions and calculating Acute Physiology and Chronic Health Evaluation II and Sequential Organ Failure Assessment scores. For patients with CKD stage 5D, blood samples were collected at enrollment, prior to the initiation of any hemodialysis session during the hospital admission, to avoid confounding effects from the dialysis procedure. Information regarding COVID-19 vaccination status, baseline serum ferritin, and use of erythropoiesis-stimulating agents was also collected and is presented in Table 1.

According to the Thailand National Guidelines for COVID-19 management during the study, all patients with COVID-19 and CKD stage 5D were classified as high-risk and requiring admission for treatment

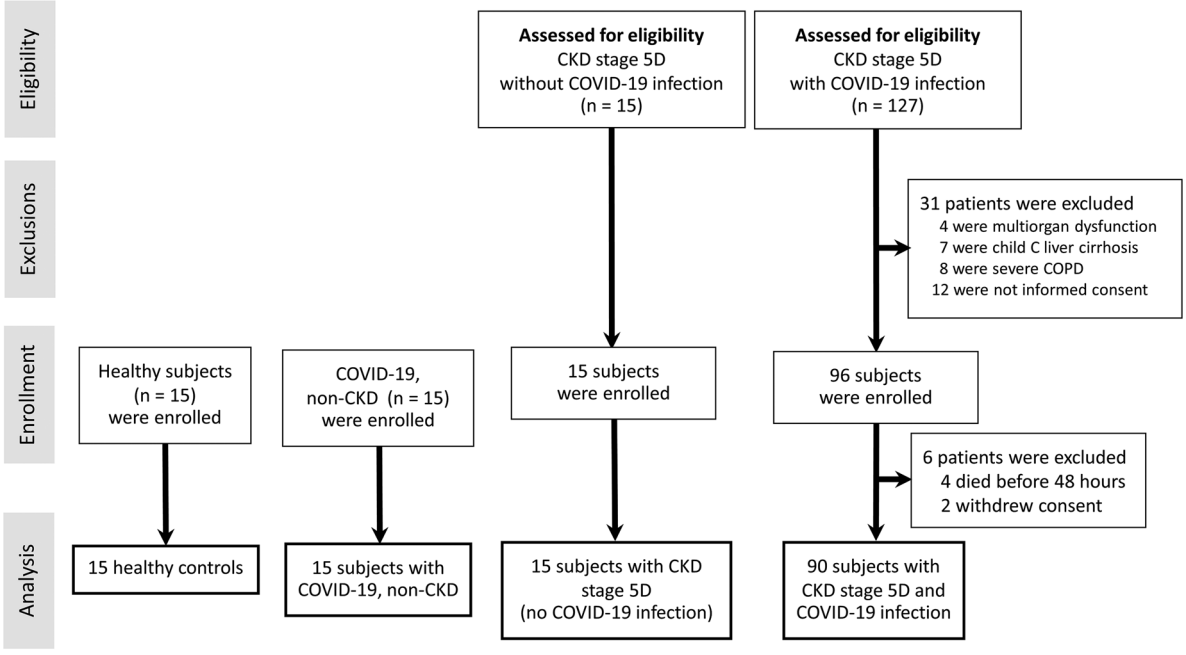

Figure 1. Study flowchart. CKD, chronic kidney disease; COPD, chronic obstructive pulmonary disease.

Table 1. Clinical characteristics of healthy and hospitalized patients with chronic kidney disease stage 5 with dialysis dependence (CKD 5D) with or without COVID-19.

	Study group ($n=135$)							
				CKD 5D with COVID-19 ($n=90$)				
Characteristic(s)	Healthy volunteers ($n=15$)	COVID-19 without CKD ($n=15$)	CKD 5D without COVID-19 ($n=15$)	Total ($n=90$)	Minimal infiltration by chest radiography ($n=14$)	<50% infiltration by chest radiography ($n=16$)	>50% infiltration by chest radiography ($n=60$)	*P*-value
Age (years)	44.3 ± 11.2	38.6 ± 10.5	48.8 ± 12.9	52.8 ± 13.4	38.3 ± 14.9	41.8 ± 16.4	52.8 ± 11.7	0.283[b]
Male	10 (66.7)	8 (53.3)	9 (60.0)	56 (62.2)	10 (71.4)	12 (75.0)	34 (56.7)	0.871[b]
BMI (kg/m^2)	22.2 ± 4.1	23.9 ± 3.1	24.2 ± 3.8	23.5 ± 3.4	23.4 ± 3.8	23.8 ± 2.7	24.2 ± 3.6	0.512[b]
Diabetes mellitus		2 (13.3)	14 (93.3)	71 (78.9)	8 (57.1)	11 (68.8)	52 (86.7)	0.293[a]
Hypertension		3 (20.0)	15 (100.0)	90 (100.0)	14 (100.0)	16 (100.0)	60 (100.0)	
COVID-19 vaccination (≥2 doses)	15 (100.0)	15 (100)	15 (100)	90 (100)	14 (100.0)	16 (100.0)	60 (100.0)	
Charlson comorbidity index		1 (0–2)	5 (4–6)	6 (4–7)	6 (4–7)	6 (4–7)	6 (4–7)	0.331[b]
APACHE II score		N/A	N/A	13 (9–17)	12 (9–16)	13 (9–17)	13 (9–17)	
SOFA score		N/A	N/A	4 (3–5)	3 (2–5)	4 (3–5)	4 (3–5)	
High-flow oxygenation ventilation		0 (0)	0 (0)	40 (44.4)	2 (14.3)	16 (100.0)	22 (36.7)	
Invasive mechanical ventilation		0 (0)	0 (0)	38 (42.2)	0 (0)	0 (0)	38 (63.3)	
28-day survival		15 (100.0)	15 (100.0)	69 (76.7)	14 (100)	13 (81.3)	42 (70.0)	0.037[a]
Laboratory findings								
PaO_2:FiO_2	N/A	N/A	N/A	198.3 ± 52.9	234.7 ± 21.9	208.8 ± 42.9	118.8 ± 38.9	
WBC (×10^9/L), mean ± SD	7.8 ± 1.5	6.7 ± 3.7	4.4 ± 2.8	5.5 ± 3.9	3.8 ± 2.2	7.7 ± 2.9	6.2 ± 5.4	0.199[b]
Platelet count (×10^9/L), mean ± SD	412.8 ± 78.2	235.5 ± 96.7	254.1 ± 63.2	215.5 ± 93.9	230.8 ± 60.9	377.7 ± 72.9	166.2 ± 55.1	0.054[b]
C-reactive protein (mg/L)	1.2 (0.3–1.6)	15.9 (5.8–55.7)	23.7 (11.7–110.4)	206.6 (65.4–300.4)	133.7 (50.9–180.4)	188.1 (94.8–234.9)	243 (104.8–338.4)	<0.0001[b]
Procalcitonin (ng/mL)	0.02 (0.01–0.03)	0.33 (0.12–1.21)	0.6 (0.3–1.58)	2.21 (0.88–4.81)	1.85 (0.71–1.89)	1.99 (0.69–3.38)	2.34 (0.99–5.88)	<0.0001[b]
D-dimer (μg/mL)	0.11 (0–0.23)	0.32 (0.26–1.59)	0.41 (0.13–1.25)	3.88 (0.44–6.26)	0.81 (0.31–1.69)	2.35 (0.88–4.12)	4.58 (0.62–6.77)	<0.0001[b]
Ferritin (ng/mL)[c]	N/A	188.2 (95.3–311.5)	450.7 (299.8–764.2)	988.4 (543.1–1560.7)	855.4 (510.2–1050.6)	992.1 (598.5–1410.2)	1145.8 (685.3–1620.4)	<0.0001[b]
Erythropoiesis-stimulating agent	0 (0)	0 (0)	13 (86.7)	78 (86.7)	12 (85.7)	14 (87.5)	52 (86.7)	1.000[a]
Corticosteroid treatment	0 (0)	1 (6.7)	2 (13.3)	90 (100)	14 (100)	16 (100)	60 (100)	<0.0001[a]
Anticoagulant treatment	0 (0)	4 (26.7)	4 (26.7)	88 (98.8)	12 (85.7)	16 (100)	60 (100)	<0.0001[a]
Vasoactive treatment	0 (0)	0 (0)	0 (0)	59 (65.6)	0 (0)	11 (68.8)	48 (80.0)	<0.0001[a]
Antibiotic treatment	0 (0)	0 (0)	0 (0)	80 (88.9)	4 (28.6)	16 (100)	60 (100)	<0.0001[a]

Data are median (IQR), *n* (%), or mean ± SD.

APACHE II: Acute Physiology and Chronic Health Evaluation II; BMI: body mass index; CKD: chronic kidney disease; N/A: not available; PaO_2:FiO_2, ratio of the partial pressure of arterial oxygen to the fraction of inspired oxygen; SOFA: Sequential Organ Failure Assessment; WBC: white blood cell count.

[a]Fisher's exact tests and [b]Mann-Whitney U tests were used to evaluate the differences between CKD 5D without COVID-19 and CKD 5D with COVID-19.

[c]Ferritin levels were not available for all patients. Data reflects the number of patients for whom laboratory results were available: Healthy volunteers (0%, $n=0$), COVID-19 without CKD (52%, $n=8$), CKD 5D without COVID-19 (38%, $n=6$), and CKD 5D with COVID-19 (48%, $n=43$).

with ≥5 days of intravenous remdesivir (200 mg from the first day, and 100 mg daily thereafter), as well as other supportive treatments, including hemodialysis, until dischargeable. Hence, patients with COVID-19 and CKD stage 5D were treated as in-patients for 5–10 days. Discharge criteria were absence of fever for ≥3 days, substantial improvement in both lungs on chest radiography, and clinical remission of respiratory symptoms. No repeated throat-swab sample for SARS-CoV-2 RNA was obtained for confirmation before discharge. Patients discharged before day 28 underwent telephone follow-up, during which survival information was recorded. All patients with severe COVID-19 and CKD stage 5D were treated in the ICU. During the study period, heparin was considered to bind to COVID-19 spike proteins and inhibit interleukin-6 (IL-6) [24], a pro-inflammatory cytokine elevated in patients with COVID-19 [25]; therefore, low-molecular weight heparin (LMWH) was administered to admitted patients, consistent with previously proposed D-dimer cutoff levels [26]. Briefly, LMWH 40 mg daily, 40 mg twice a day, and 1 mg/kg (maximum 60 mg) twice a day were prescribed for patients with COVID-19 and circulating D-dimer levels <0.5,

0.5–3, and >3 µg/mL, respectively. Patients who received LMWH continued anticoagulation following hospital discharge, unless contraindicated.

Density gradient cell separation

PBMC and PMN fractions were isolated from heparin-anticoagulated blood by density gradient cell separation. Samples were layered onto Ficoll-Paque (Robbins Scientific Corporation, Sunnyvale, CA, USA) and Polymorphprep™ (Axis-Shield, Oslo, Norway) in a 1:1:1 ratio in 50 mL sterile tubes and centrifuged (400*g*, 35 min, room temperature). The PMN layer, largely comprising neutrophils (>95%), was removed, washed with RPMI 1640 (Thermo Fisher Scientific, Logan, Utah, USA), and resuspended in RPMI 1640 supplemented with 10% heat-inactivated fetal bovine serum. Contaminating erythrocytes were removed using ammonium chloride lysis buffer. Neutrophil preparations were ≥95% viable and pure, as confirmed by trypan blue exclusion (Sigma-Aldrich, Singapore) and Wright's Giemsa staining (Biotech, Bangkok, Thailand), respectively. LDGs were isolated from the PBMC fraction and stained with Wright's Giemsa stain. Cells were counted by light microscopy.

Serum sample analysis

Serum cytokines (TNF-α, IL-6, IL-8, and IL-10) and endotoxin (lipopolysaccharide; LPS) were measured by enzyme-linked immunosorbent assay (ELISA) (Invitrogen, Waltham, MA, USA) and human embryonic kidney (HEK)-Blue LPS Detection Kit 2 (InvivoGen™, San Diego, CA, USA), respectively. HEK-Blue cells (1×10^5/well) were added into 96-well plates with serum samples and standard LPS before incubation overnight at 37 °C in 5% CO_2. Then, 180 µL QUANTI-Blue was added and incubated for 1 h before reading absorbance at 620 nm using a fluorescent microplate reader (Bio-Tek, Winooski, VT, USA). Serum cell-free DNA was measured using Quant-iT™ PicoGreen reagent (Thermo Fisher Scientific, Paisley, UK) on a fluorescent microplate reader (Bio-Tek) at 480/520 nm, according to the manufacturer's instructions. Levels of CitH3 were measured by ELISA kit (Roche, Mannheim, Germany).

NETs formation detection

Neutrophils (5×10^5/well) were incubated in RPMI 1640 for 1 h at 37 °C before adding onto poly-L-lysine-coated glass coverslips (6 mm diameter) (Sigma-Aldrich), fixing with 4% (v/v) formaldehyde, blocking with tris-buffered saline (TBS) in 2% (w/v) bovine serum albumin (Sigma-Aldrich), and permeabilizing using TBS with 0.05% Tween 20 (Sigma-Aldrich). NET formation was detected by analysis of nuclear morphology using 4′,6-diamidino-2-phenylindole (DAPI) staining or co-immunofluorescence staining with myeloperoxidase (MPO) and neutrophil elastase (NE) (Abcam, Cambridge, UK). Then, ProLong antifade medium (Invitrogen) was added, and cover slips with cells mounted upside down before visualizing by confocal microscopy. Percentages of cells with NETs among all strained cells represented the NET formation level.

NETs were also assessed by determining the expression levels of several genes by real-time PCR. RNA was extracted from neutrophil pellets using a FarvoPrep RNA mini kit (Farvogen, Vienna, Australia), quantified using a NanoDrop OneC Microvolume UV-Vis Spectrophotometer (Thermo Scientific) and reverse-transcribed (Applied Biosystems, Warrington, UK), before analysis using an Applied Biosystems QuantStudio 6 Flex Real-Time PCR System with SYBR® Green PCR Master Mix (Applied Biosystems) and the primers listed in Table 2. Results are presented as relative quantitation using the comparative threshold method ($2^{-\Delta\Delta Ct}$) and normalized to β-actin levels.

Ex vivo experiments

Gradient separated neutrophils (1×10^7) were incubated with LPS (*Escherichia coli* 026: B6; Sigma-Aldrich) at 100 ng/mL or culture media (RPMI) before another gradient separation to isolate LPS-derived LDGs and LPS-derived neutrophils of regular density. Then, cells were stained with fluorochrome-conjugated

Table 2. Primers.

Name	Forward primer	Reverse primer
Extracellular signal-regulated kinases 1 (*ERK1*)	5′-TGGCAAGCACTACCTGGATCAG-3′	5′-GCAGAGACTGTAGGTAGTTTCGG-3′
Peptidyl arginine deiminase 4 (*PAD4*)	5′-CGAAGACCCCCAAGGACT-3′	5′-AGGACAGTTTGCCCCGTG-3′
Protein kinase C (*PKC*)	5′-GAGGGACACATCAAGATTGCCG-3′	5′-CACCAATCCACGGACTTCCCAT-3′
β-actin	5′-CCTGGCACCCAGCACAAT-3′	5′-GCCGATCCACACGGAGTACT-3′

antibodies against CD11b, CD62, CD63, and CD66b, and analyzed by flow cytometry [27]. Cells were resuspended in binding buffer (1×10^6 cells/100 µL) for 15 min before analysis with BD LSR-II (BD bioscience) using FlowJo software version 10.

Plasma coagulation factor assays

ELISA kits (R&D Systems, Minneapolis, MN, USA) were used to measure soluble PF4 and RANTES levels in plasma samples from patients with COVID-19 and healthy donors. von Willebrand factor (vWF) antigen and D-dimers were analyzed in identical samples using ELISA kits (Abcam, Cambridge, United Kingdom).

Outcomes

The primary outcome was to assess a difference in NETs and LDGs concentrations between COVID-19 cases with versus without CKD stage 5D along with CKD stage 5 D and healthy controls. Key secondary outcome measures reported here were to assess associations between NETs and LDGs concentrations and other clinical COVID-19 severity spectrums, immune and cytokine mediators, microthrombi formation and platelet deposition, and 28-day mortality.

Statistical analysis

Data are presented as mean ± standard deviation (SD) and percentage. Categorical variables were assessed using Fisher's exact test, and continuous variables using Mann-Whitney *U*. We performed correlation analyses of both NETs and LDGs with clinical spectrums and performed survival analyses with a log-rank test stratifying patients according to high or low concentrations of NETs and LDGs. All statistical analyses were performed with GraphPad Prism version 10.1.2 (GraphPad software, Inc, San Diego, CA, CA, USA). $p < 0.05$ was considered statistically significant.

Results

Patient demographic and clinical characteristics

A total of 135 participants were enrolled, with slightly more male than female participants in all groups. Of 127 eligible patients with CKD stage 5D hospitalized with COVID-19 infection, 90 cases with complete data and defined outcomes were included, among which 60 cases (66.7%) were severe. COVID-19 infection severity was classified according to chest radiography, with >50% lung infiltration indicating severe COVID-19 infection [22]. Patients with severe disease had a higher mortality rate (21.7%) than those with non-severe disease (6.2%). All patients with severe disease received anticoagulant treatment, as either prophylaxis ($n = 11$, 18.3%) or treatment ($n = 49$, 81.7%). Participant classifications, and demographic and clinical characteristics are shown in Figure 1 and Table 1.

CKD stage 5D interferes with certain COVID-19 severity parameters

Our primary interest was in the impacts of COVID-19 in patients with CKD stage 5D; however, concerns about the interference of CKD stage 5 in cases with severe COVID-19 infection led to us to conduct an initial comparison between cases with versus without CKD stage 5D. NETs, evaluated by assessment of nuclear morphology using DAPI staining, were increased in patients with severe COVID-19 infection,

regardless of CKD stage 5D, while CKD stage 5D alone did not lead to NETs elevation (Figure 2A,B); however, detection of NET formation based on other parameters, including serum CitH3, expression of NETs-associated genes (*PAD4*, *ERK1*, and *PKC*), and low-density granulocytes, did not differ among groups (Figure 2C–G). In contrast, elevated endotoxemia was detected only in patients with CKD stage 5D and severe COVID-19, but not in other groups, including patients with severe COVID-19 without CKD stage 5D (Figure 2H), while serum cell-free DNA was increased in all groups, except for healthy controls (Figure 2I). Further, pro-inflammatory (TNF-α, IL-6, and IL-8), but not anti-inflammatory (IL-10), cytokines were higher in all groups of patients (non-CKD stage 5D with COVID-19 and CKD stage 5D regardless of COVID-19) than in healthy controls (Figure 2J–M). Thus, CKD stage 5D without COVID-19 induced elevation of serum pro-inflammatory cytokines and cell-free DNA, but not endotoxemia and NETs (detected using DAPI) (Figure 2A–M).

NETs and LGDs as prognostic biomarkers in patients with CKD stage 5D and COVID-19 infection with severe pulmonary involvement

To determine the possible influence of CKD stage 5D in the context of COVID-19, all parameters were measured next in cases with CKD stage 5D without COVID-19. COVID-19 severity was categorized according to chest radiography criteria as minimal, $<50\%$, or $>50\%$ infiltration [22]. Patients with COVID-19 and high infiltration were further categorized as those breathing room air, or with high flow nasal canular- or invasive mechanical ventilator-assisted (IMV) breathing. Among CKD stage 5D patients, NETs detected by DAPI staining were highest in those with severe COVID-19 infection (chest radiography criteria), particularly those with IMV support (Figure 3A,B), implying that NETs have potential as predictors of IMV support or subsequent severe respiratory failure; however, NETs measured by serum CitH3 and gene expression levels did not differ between patients with CKD stage 5D and controls (Figure 3C–F). Despite the lack of difference between patients with CKD stage 5D and controls, *PAD4* expression was higher in patients with severe COVID-19 receiving IMV support than in those without ventilator assistance (Figure 3D, inset). LDGs were similarly elevated in patients with COVID-19 independent of its severity; however, LDGs were higher in patients receiving IMV support than in those with high infiltration without IMV support (Figure 3G). Endotoxemia, cell-free DNA, and serum cytokines did not differ between CKD stage 5 controls versus those with COVID-19 infection (Figures 3H–G and 4A–D). In patients with COVID-19 and high infiltration, serum IL-6 was higher in those receiving than in those without IMV support (Figure 4B, inset). Hence, LDGs and serum IL-6 may be useful indicators for predicting ventilator support in patients with CKD stage 5D and COVID-19 infection. Although there was no significant correlation between either LDGs or NETs and all patients with CKD stage 5D and COVID-19 infection, a significant correlation was detected in cases with severe lung infiltration (Figure 4E,F). Notably, both NETs and LDGs could predict severe lung injury determined by the ratio of the partial pressure of arterial oxygen to the fraction of inspired oxygen ($r=0.6971$, $p<0.0001$ and $r=0.318$, $p<0.013$, respectively) and survival (both $p<0.0001$), particularly in patients with severe lung injury (Figure 4G–J, H, insets). There was significant difference in mortality in patients with COVID-19 with higher NETs (morphology by DAPI) and LDGs percentages compared with those with low percentages ($p=0.0007$ and $p=0.017$, respectively) (Figure 4I,J).

NETs are associated with microthrombi formation and platelet deposition in CKD stage 5D with COVID-19

To ascertain the pathogenesis underlying microthrombi resulting from NETosis in patients with advanced CKD infected and COVID-19, we investigated levels of the circulating thrombotic markers, vWF and D-dimers, in these patients relative to those in patients with CKD stage 5D without COVID-19. Circulating D-dimer and vWF concentrations were significantly elevated in patients with stage 5D CKD and COVID-19 (both $p<0.0001$; Figure 5A,B); however, no direct correlations between these parameters and NETs or LDGs were observed in our cohort (data not presented). Similarly, we detected substantially increased concentrations of soluble platelet-derived factors that induce NETosis, including PF4 and RANTES, in patients with stage 5D CKD and COVID-19 (both $p<0.0001$; Figure 5C,D).

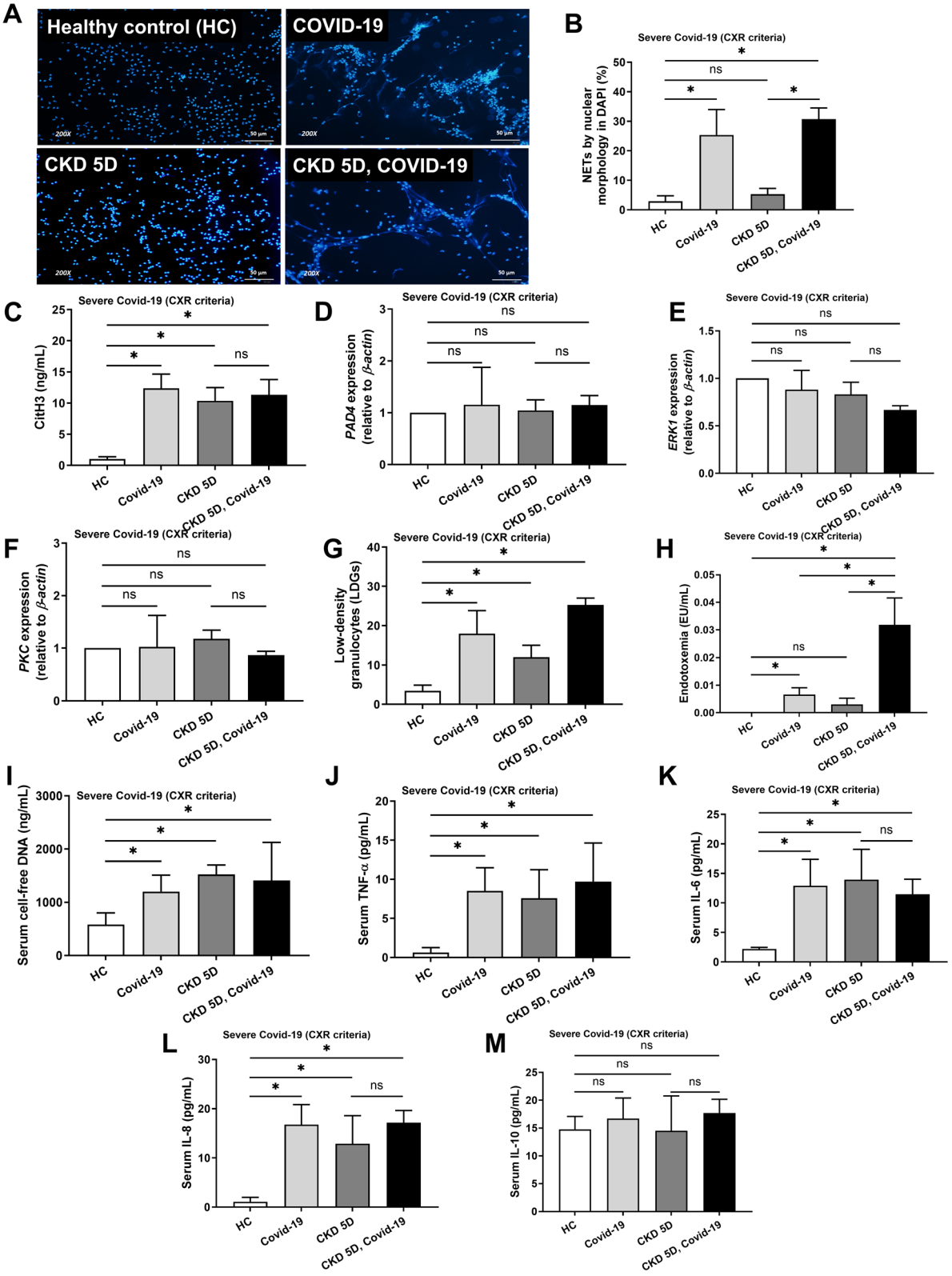

Figure 2. Analysis of NETs and LDGs in all study participants. Characteristics of healthy controls ($n = 15$), and patients with COVID-19 without CKD ($n = 15$), CKD stage 5D alone ($n = 15$), and CKD stage 5D with COVID-19 infection ($n = 90$), including neutrophil extracellular traps (NETs) assessed by analysis of nuclear morphology using DAPI fluorescent staining (%) (representative images, (A) quantification, (B), serum citrullinated H3 (CitH3) I, expression of several genes, including peptidyl arginine deiminase 4 (*PAD4*), extracellular signal-regulated kinase 1 (*ERK1*), and protein kinase C (*PKC*) (D–F, respectively), low-density granulocytes (LDGs) (G), endotoxemia (H), serum cell-free DNA (I), and serum cytokines (TNF-α, IL-6, IL-8, and IL-10) (J–M, respectively**)**. Only patients with COVID-19 and >50% lung infiltration determined by chest radiography (severe COVID-19 by chest radiography (CXR) criteria) were included. *$p < 0.05$ between the indicated groups; ns: not significant.

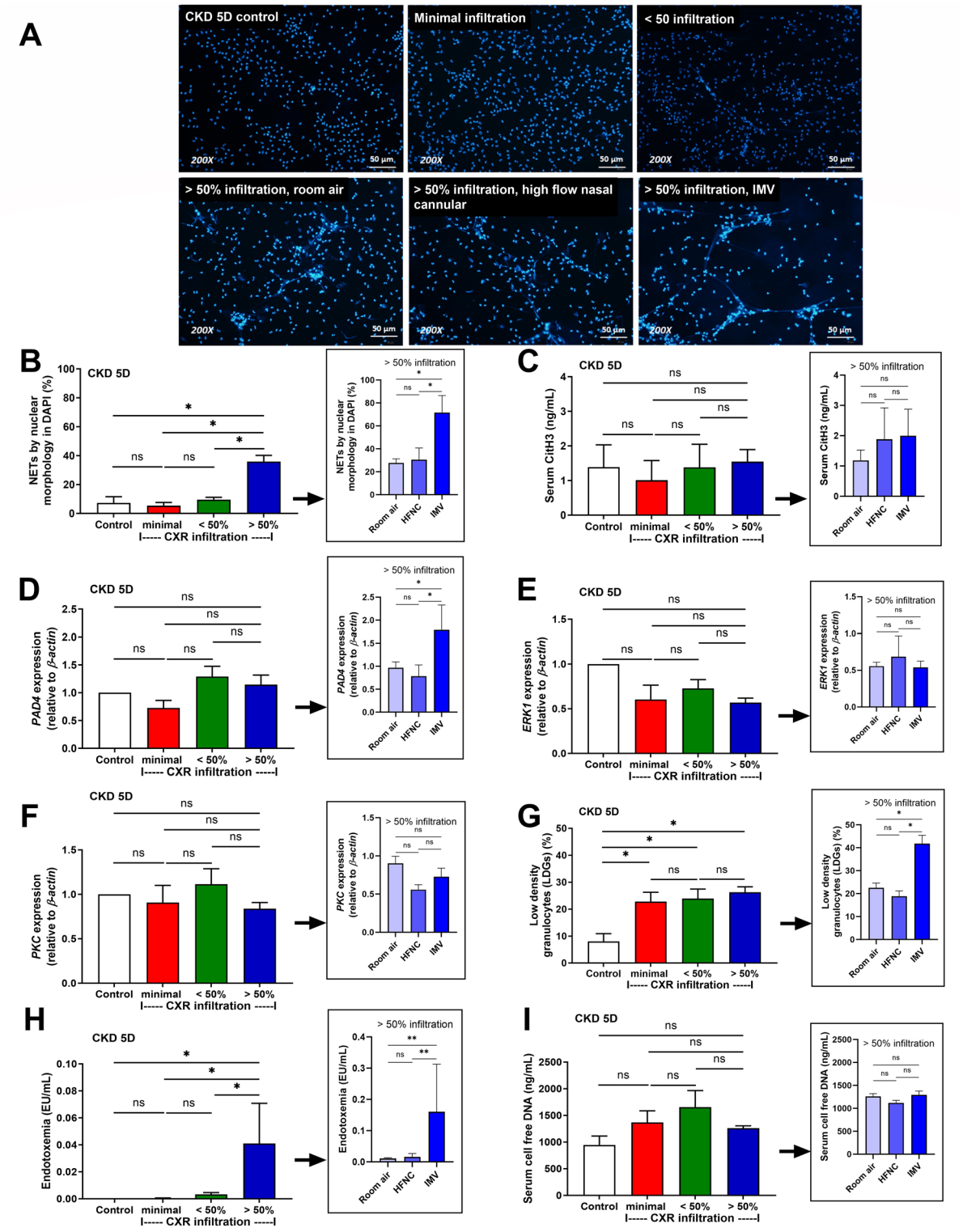

Figure 3. Analysis of NETs and LDGs in patients with CKD stage 5 without COVID-19 and with COVID-19 of differing severity. COVID-19 severity was categorized according to chest radiography criteria as minimal, <50%, or >50% infiltration [19]. Characteristics of patients with CKD stage 5 without COVID-19 (control) ($n = 15$), and with COVID-19 and different chest radiograph (CXR) findings, including minimal ($n = 14$), <50% ($n = 16$), and >50% infiltration ($n = 60$), together with Sub-group analysis of patients in the >50% infiltration group classified as cases breathing room air ($n = 40$), or receiving high flow nasal cannular (HFNC, $n = 10$), or invasive mechanical ventilator (IMV, $n = 10$) (inset graphs). Parameters measured were: neutrophil extracellular traps (NETs) assessed by nuclear morphology using DAPI fluorescent staining (%) (representative images, A; quantification, B), serum citrullinated H3 (CitH3) ©, expression of several genes, including peptidyl arginine deiminase 4 (*PAD4*), extracellular signal-regulated kinase 1 (*ERK1*), and protein kinase C (*PKC*) (D–F, respectively), low-density granulocytes (LDGs) (G), endotoxemia (H), and serum cell-free DNA (I). *$p < 0.05$ between the indicated groups; ns: not significant.

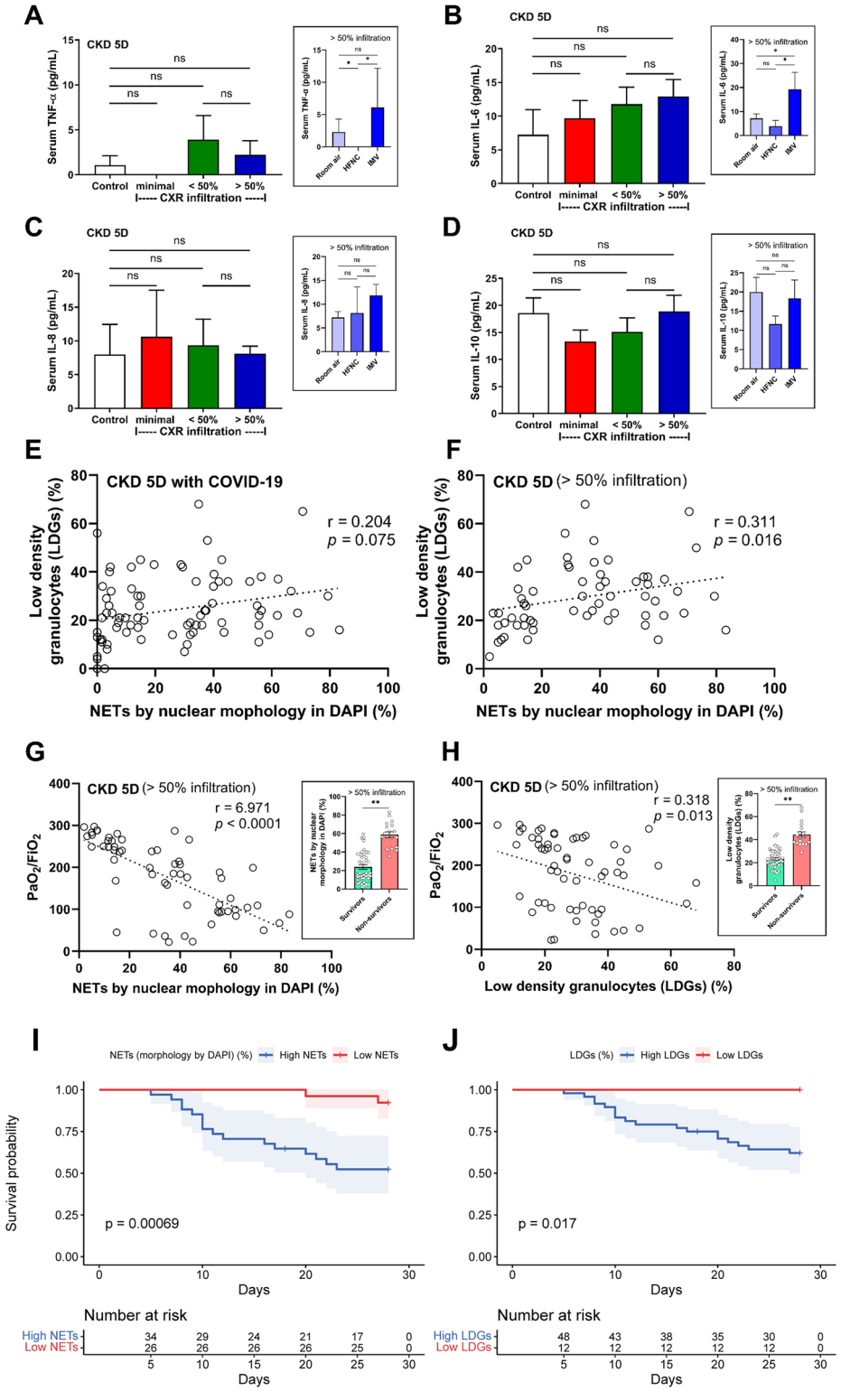

Figure 4. NETs And LDGs to predict severe lung injury and survival in patients with CKD stage 5D and COVID-19. Characteristics of cases with CKD stage 5D without (control; $n=15$), and with COVID-19 and different chest radiograph (CXR) findings, including minimal ($n=14$), <50% ($n=16$), and >50% infiltration ($n=60$), together with the Sub-group analysis of the >50% infiltration group into cases breathing room air ($n=40$), or receiving high flow nasal canular (HFNC, $n=10$) and invasive mechanical ventilator (IMV, $n=10$) (inset graphs). Parameters measured were: levels of serum cytokines (TNF-α, IL-6, IL-8, and IL-10) (A–D, respectively) and correlation between low-density granulocytes (LDGs) versus neutrophil extracellular traps (NETs) among all cases with CKD stage 5D (E) and those with CKD stage 5D and >50% lung infiltration (F). Notably, both NETs (G) and LDGs (H) potentially predict severe lung injury and survival (insets). Kaplan-Meier analysis for 28-day mortality of CKD stage 5D cases with COVID-19 with NETosis (morphology by DAPI) and LDGs analyses, stratified by high- and low-NETs versus high- and low-LDGs (cutoff at 41.5% for NETs and at 17.9% for LDGs, as defined by median). Log-rank test was used to compare survival distribution (I, J). *$p<0.05$ and **$p<0.0001$ between the indicated groups; ns: not significant.

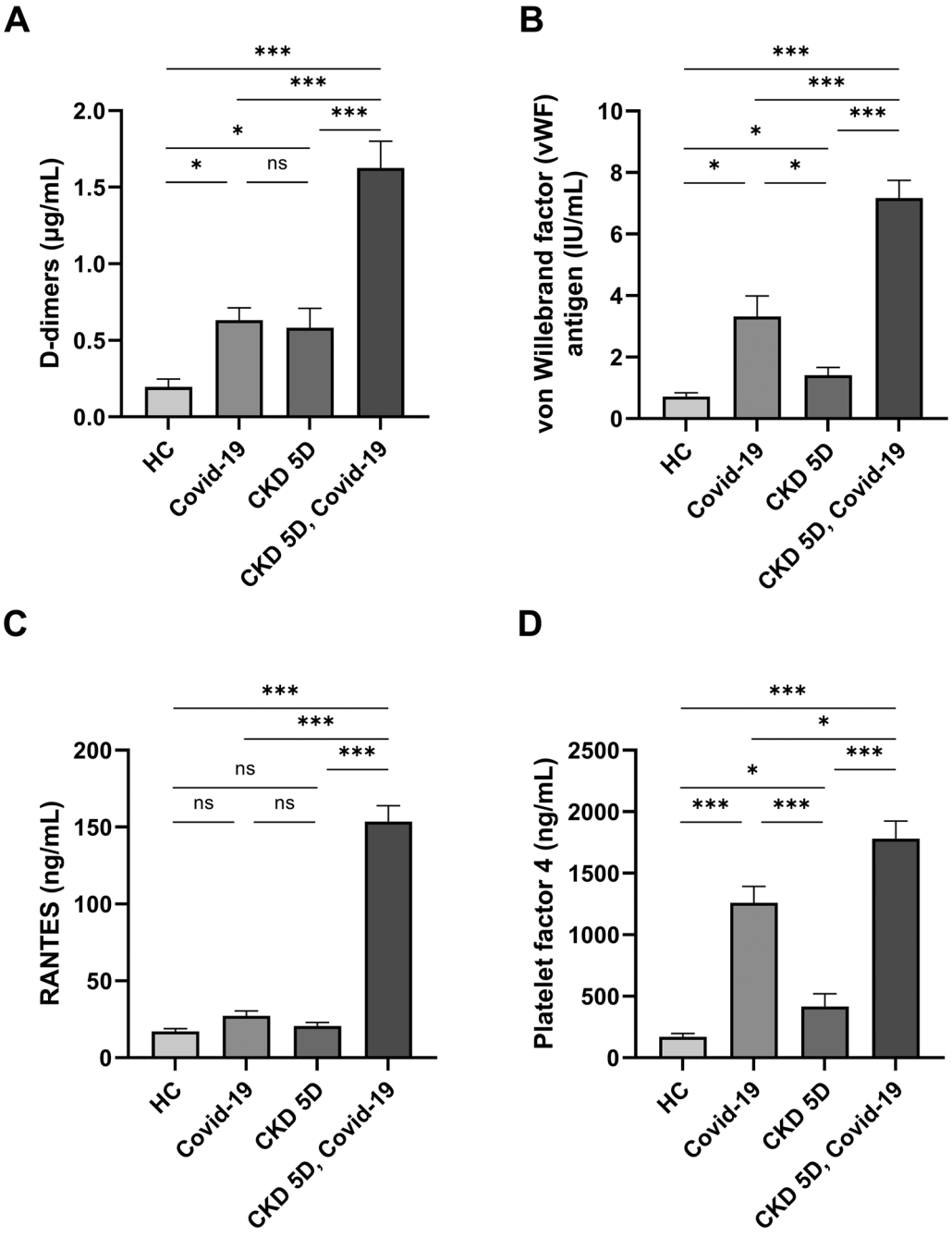

Figure 5. NETs Are associated with microthrombi formation and platelet deposition. Plasma levels of D-dimers (a), von willebrand factor (vWF) (B), RANTES (C), and platelet factor 4 (PF4) (D) quantified by ELISA in patients with CKD stage 5D and COVID-19 compared with those without COVID-19 and healthy controls. *$p < 0.001$ and ***$p < 0.0001$ between the indicated groups; ns: not significant.

Endotoxemia during COVID-19 in CKD stage 5D may induce LDGs

To determine possible sources of LDGs during active inflammatory conditions, neutrophils were separated from healthy controls before stimulation with LPS, and their density assessed by gradient separation, before retrieving low (LPS-LDGs) and normal (LPS-neutrophils) density LPS-stimulated cells (Figure 6A). LPS-activated neutrophils transformed into LDGs in a time-dependent manner, as approximately 30% and 70% of stimulated cells were LDGs at 1 and 2 h post-activation (Figure 6B). Separated neutrophils not stimulated using LPS (unstimulated neutrophils) retained their high density, demonstrating that the separation method did not induce LDG generation (Figure 6B). Next, we evaluated several flow cytometry parameters, including CD62 (the adhesion molecule, selectin), CD63 (a member of the

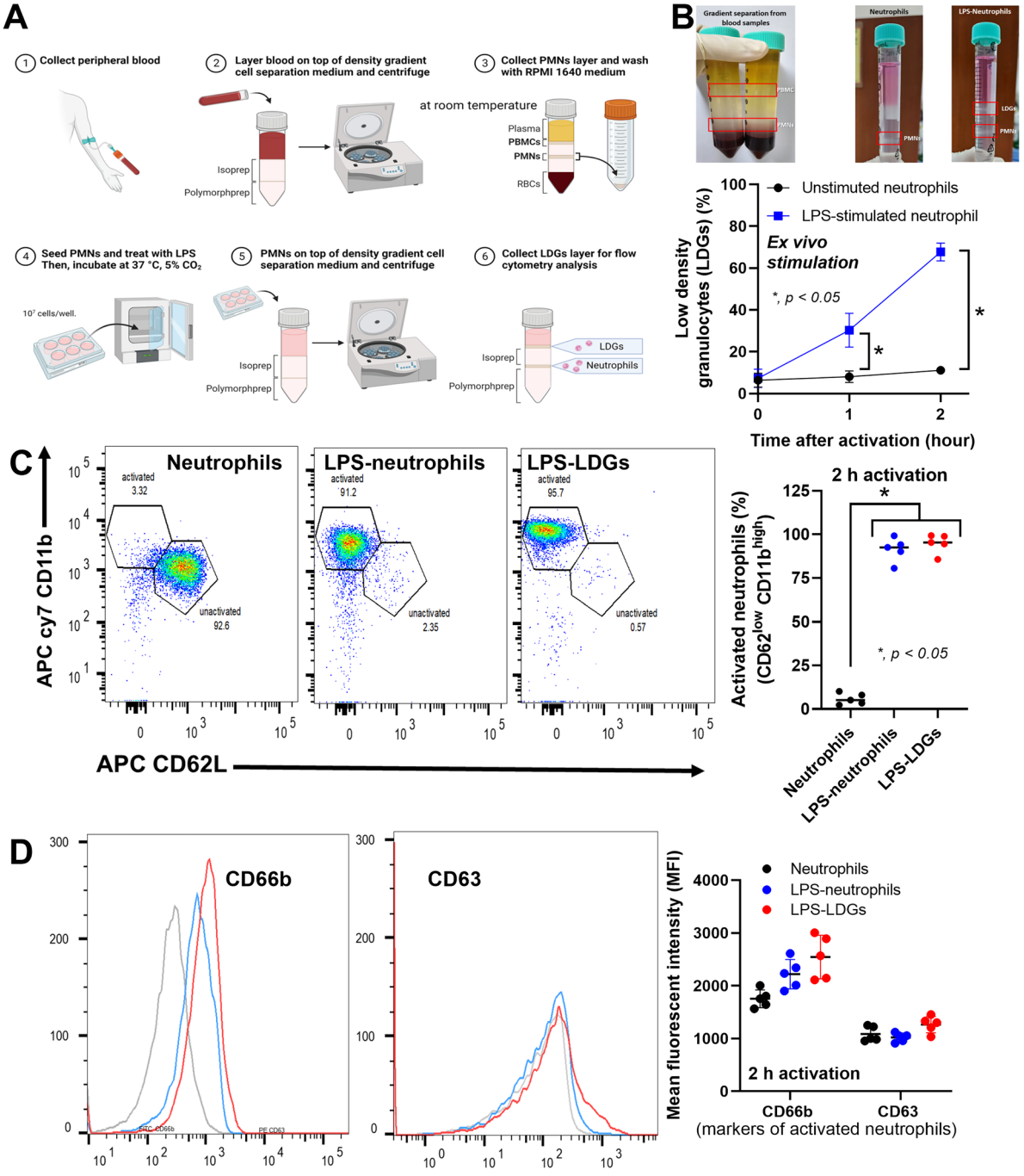

Figure 6. Study overview. (A) Schema of the experiments showing blood collection ①, centrifugation ②, separation into different layers, including plasma, peripheral blood mononuclear cells (PBMCs), polymorphonuclear cells (neutrophils; PMNs), and red blood cells (RBC), by gradient separation and collection of PMN using RPMI media ③, and LPS activation ④, before additional separation ⑤ to identify LPS-stimulated cells with low (LPS-LDGs) and normal (LPS-neutrophils) density ⑥. Characteristics of neutrophils from processes ③ (non-activated neutrophils) and ⑥ (LPS-LDGs and LPS-neutrophils) in the schema, indicated by LDG percentage (number of LPS-LDGs/number of LPS-LDGs + LPS-neutrophils) with the representative images of gradient separation (B), markers of neutrophil activation ($CD62^{low}$ $CD11b^{high}$) and neutrophil degranulation (CD66b and CD63) with representative flow cytometry patterns (C, D). Results were derived from separate experiments conducted in triplicate. *$p < 0.05$ between the indicated groups. LDG: low density granulocytes; LPS: lipopolysaccharides (endotoxins).

transmembrane 4 superfamily), CD11b (complement receptor 3), and CD66b (carcinoembryonic antigen-related cell adhesion molecule 8), in neutrophils, LPS-LDGs, and LPS-neutrophils (Figure 6C,D). Unlike regular neutrophils, both LPS-LDGs and LPS-neutrophils were $CD62^{low}$ $CD11b^{high}$ (Figure 6C), while CD66b and CD63 (degranulation markers) did not differ among groups (Figure 6D). Hence, the lower

density of neutrophils after activation could not be explained by de-granulation. Due to possible NETs formation in LDGs, we next detected NETs before and after LPS stimulation using immunofluorescent MPO (red color) and NE (green color) staining. Cells generating extracellular traps (ETs), indicated by MPO and NE staining and fiber-liked structure, were detected in patients with severe COVID-19 breathing either room air or with ventilator assistance (Figure 7A,B). Further, LPS induced a higher percentage of cells with ETs only in samples from patients breathing room air, but not in those from patients receiving ventilator assistance (Figure 7A,B). Thus, most LDGs from patients with profoundly severe COVID-19 (cases with ventilator-assisted breathing) may have already generated ETs, while not all LDGs from less severe cases (breathing room air) generated ETs (Figure 7A,B). Thus, ETs levels in PBMCs may be associated with COVID-19 severity.

Discussion

Unlike most viral respiratory infections, COVID-19 infects various non-respiratory cells, leading to systemic inflammatory responses [28], similar to the impacts of accumulated uremic toxins in patients with CKD stage 5 [29,30]. The intestine is among several organs that can be disrupted by both SARS-CoV-2 and uremic toxins, as indicated by endotoxemia from gut barrier defect reported in patients with both COVID-19 [31,32] and CKD stage 5D [33,34]. Endotoxins are major components of Gram-negative bacteria, which are the most abundant microbes in the gut. Endotoxemia without active systemic bacterial infection is an indirect biomarker of gut barrier defect, while profound inflammatory responses against SARS-CoV-2-infected cells [35] and uremic toxin-induced oxidative stress [36], contribute to systemic inflammation, with severe responses leading to death of immune and other cells and elevated cell-free DNA [37,38]. Although the systemic biomarkers of less severe COVID-19 do not overlap with those of CKD stage 5D [39–41], some parameters in severe COVID-19 exhibit similarities to CKD stage 5D. The disease conditions can be distinguished from healthy controls using cell-free DNA, serum cytokines (TNF-α, IL-6, and IL-8), LDGs, and NETs (analyzed using CitH3); however, similar levels are found in patients with COVID-19 with and without CKD stage 5D and those with CKD stage 5D alone. Similarly, the pronounced elevation of ferritin in our cohort is consistent with the hyperferritinemia characteristic of severe COVID-19 [42], where it acts not just as a marker of inflammation but as a potential pro-inflammatory mediator that could contribute to the pathology promoting NETs and LDGs. Notably, NET levels determined using gene expression did not differ between patients and healthy controls and the inconsistency in the differences in NETs parameters between patients with CKD stage 5D (low level of DAPI-stained NETs, but high levels of serum CitH3) indicates some limitations to this approach. Neutrophil phenotype can be influenced by various factors, including heterogeneity among patient cohorts under investigation (e.g., comorbidities, medications like the near-universal use of erythropoiesis-stimulating agents in the CKD groups, and the etiology of CKD) [43–45]. More robust clinical trials are required to determine whether and how the capacity for NETs formation is affected in CKD.

NETs assessed by DAPI staining have been considered a gold standard parameter, while serum CitH3 may be more clinically useful. Factors contributing to the variation in conclusions regarding the ability of neutrophils isolated from patients undergoing dialysis to form NETs remain unknown. Meanwhile, we found that endotoxemia was elevated only in patients with CKD stage 5D and severe COVID-19, but not those with CKD stage 5D alone, perhaps depending on uremia severity. Notably, all patients with CKD stage 5D alone in this study underwent online hemodiafiltration, a method that has potential to reduce endotoxin levels [46,47]. Hence, there was some overlap between CKD stage 5D and severe COVID-19 infection and data from patients with CKD stage 5D and COVID-19 infection warrants further exploration.

Except for NETs and LDGs, most parameters analyzed could not distinguish between CKD stage 5D and CKD stage 5D with COVID-19, highlighting the impact of neutrophil activation during COVID-19 infection. Notably, NETs (assessed by DAPI and *PAD4* expression) and LDGs were highest in patients with CKD stage 5D and severe COVID-19 (breathing with respirator assistance) and only NETs assessed by DAPI could differentiate between severe versus less severe COVID-19 in patients with CKD stage 5D. Although serum CitH3 can differentiate healthy controls from patients with CKD stage 5D, it could not distinguish COVID-19 from non-COVID-19 infection among cases with CKD stage 5D. This may reflect that CitH3 was already activated by uremic toxins, but not sufficiently to alter neutrophilic nuclear

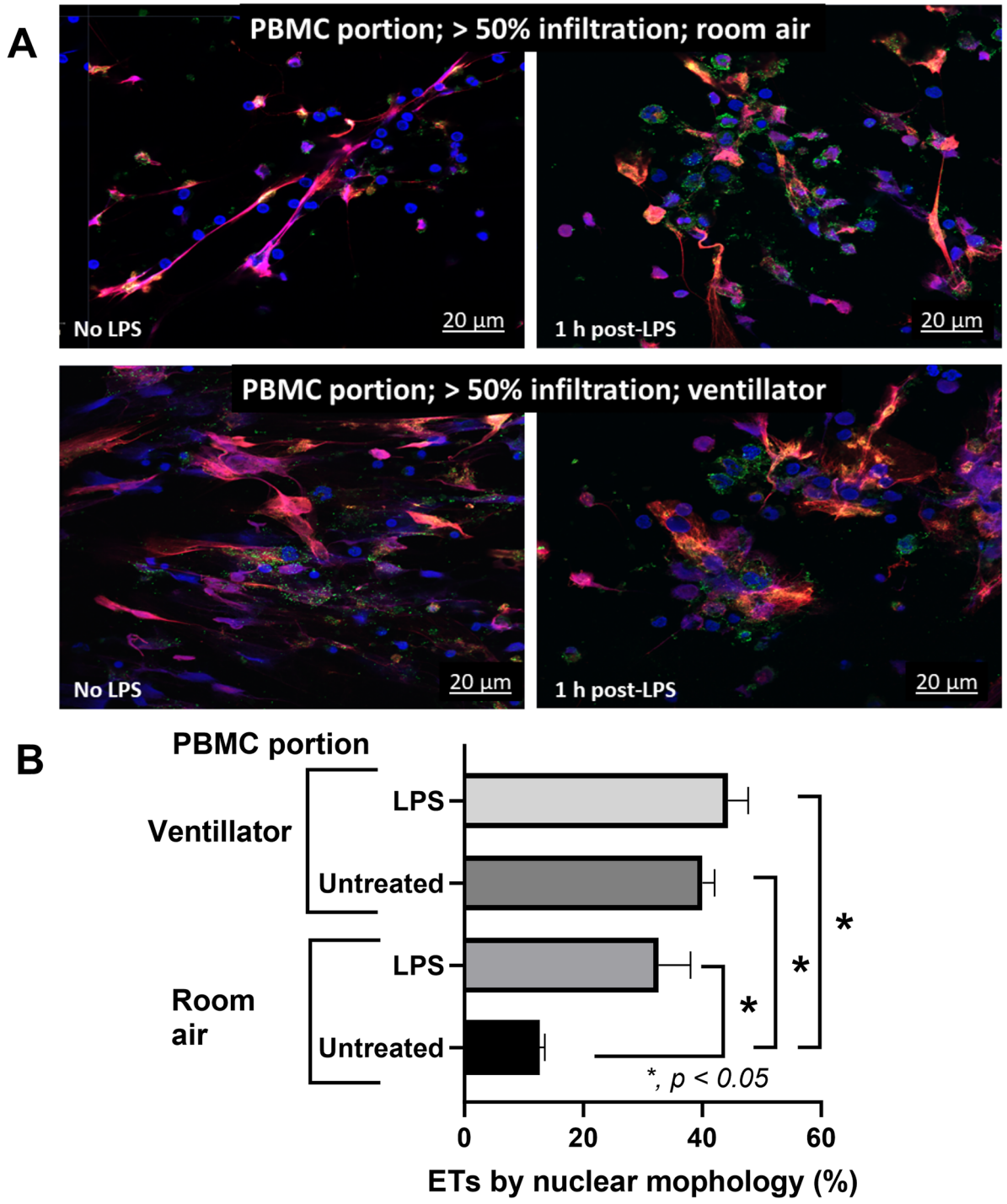

Figure 7. Characteristics of extracellular traps. Characteristics of extracellular traps, possibly from neutrophils, in the peripheral blood mononuclear cell (PBMC) fraction from patients (COVID-19 with end stage renal disease) with >50% lung infiltration who could tolerate room air or were subject to invasive mechanical ventilation (IMV; ventilator) with or without 1-h LPS stimulation, as indicated by the percentage of cells positive for anti-myeloperoxidase (MPO; red color) and anti-neutrophil elastase (NE; green color) staining; representative images are shown (A, B) ($n=7$ per group). LPS: lipopolysaccharides/endotoxin.

morphology (DAPI staining), which was induced only by uremia plus COVID-19 infection. Furthermore, almost all patients with COVID-19 in this cohort (98.8%) were administered LMWH, as either a prophylactic or treatment, to prevent thromboembolism, due to high D-dimer levels, which may also counteract the deleterious effects of histone-mediated thrombosis [48].

Due to the limited data on LDGs and elevated LDGs in COVID-19 infection, regardless of CKD stage 5D, we considered it possible that LDGs may be partly derived from the reduced density of neutrophils after stimulation. Using LPS as a representative activator, we demonstrated that LPS-activated neutrophil density of was similar to that of LGDs, as determined by gradient separation assay, and LPS could not further decrease the density of LDGs. Hence, some of the detected LDGs may be activated neutrophils, as indicated by similar flow cytometry characteristics of LDGs and activated neutrophils ($CD62^{low}$ $CD11b^{high}$). The reduced density of LDGs and LPS-activated neutrophils was not due to granule secretion, as CD66b and CD63 levels in these cells were not different from those in regular neutrophils. Hence, some LDGs may be activated neutrophils, which may generate NETs (Figure 7). Additionally, NETs in LDG fractions were higher in samples from patients with severe COVID-19 receiving ventilator assistance than the group breathing unassisted. Further, NETs were increased after LPS stimulation in LDGs from cases without breathing assistance, but not in those from patients on ventilators, implying maximal NETs in the LDG fraction in patients with CKD stage 5D and severe COVID-19.

A crucial advantage of using LDGs as a biomarker is the practicality of its measurement. The isolation of LDGs is achieved through standard density gradient centrifugation, a robust and widely available technique that requires minimal specialized equipment beyond a centrifuge. Subsequent quantification can be performed with a simple light microscope following standard cytological staining. This stands in contrast to the measurement of NETs *via* immunofluorescence, which necessitates expensive microscopy equipment and technical expertise, or serum biomarkers like CitH3, which require specific ELISA kits. The relatively low cost, rapid turnaround time, and accessibility of LDG measurement make it a particularly promising prognostic tool for predicting the need for IMV in high-risk patients, especially in resource-limited healthcare settings where advanced diagnostic platforms may not be available. Although LDGs could not differentiate between less severe and severe COVID-19, unlike NETs assessed by DAPI, initial evaluation by chest radiography plus LDGs may be an economically viable predictor of the need for IMV.

Although clinical thrombotic events were not reported in this cohort, levels of thrombotic markers, including vWF, D-dimers, RANTES, and PF4, were significantly higher in patients with COVID-19 and stage 5D CKD than in those without the virus and healthy controls. These results could potentially account for the interaction between NETs and platelets that triggers a thrombo-inflammatory cascade, resulting in the clinically observed hypercoagulability and subsequent thrombosis states associated with COVID-19. There was no correlation between plasma levels of thrombotic markers and plasma NET levels in our cohort, possibly due to disturbances induced by LMWH administration in patients infected with COVID-19. Moreover, the complex role of NETs in thrombosis could account for the lack of association between vWF and D-dimers. Initially, vWF antigen concentrations were evaluated in lieu of its activity, and it is crucial to acknowledge that vWF antigen levels do not provide an authentic representation of the capacity of vWF to interact with platelets and PMNs [49]. Activated and impaired endothelium secretes vWF, and this is anticipated to occur during the initial phases of COVID-19. We assessed plasma vWF levels during patient hospitalization, which may be during the later phase of the disease. Notably, the exceedingly high levels detected could potentially be attributed to two factors: persistent inflammation induced by NETs [50] or preexisting CKD [51]. In addition, continuous fibrinolysis generates plasma D-dimers, and clots dense in NETs are resistant to tissue plasminogen activator degradation [52]. In the absence of a correlation between D-dimers and NETs, an inability of individuals with COVID-19 to break down blood clots may be indicated. Finally, future studies for testing the activation of NETs by separating platelets (the platelet-rich plasma stimulation) might add more value to this study, particularly in CKD stage 5D patients with COVID-19.

This study has several limitations that should be acknowledged. First, its observational, single-center design may limit the generalizability of our findings, and the sample size, particularly in the sub-group analyses, was modest. Second, while we controlled many clinical variables, the possibility of unmeasured confounders remains. Furthermore, while ferritin was measured as a key inflammatory marker, the data was incomplete for a portion of the cohort, which limits the ability to draw definitive conclusions from this specific biomarker. Third, the near-universal administration of LMWH, while reflecting standard clinical practice, likely confounded our ability to detect a direct correlation between NETs and systemic thrombotic markers. Finally, we observed a notable discrepancy between different methods of NET quantification. While NETs assessed by DAPI staining correlated strongly with disease severity, soluble markers

like serum CitH3 and NET-related gene expression did not. This may reflect the complex, multi-step nature of NETosis in the setting of uremia and severe infection, where different markers may capture distinct stages of neutrophil activation, a phenomenon that warrants further investigation.

In conclusion, NETs (assessed by DAPI) and LDGs, but not serum cytokines or endotoxemia, may be useful predictors of IMV use in patients with CKD stage 5D and COVID-19 involving >50% lung infiltration. Due to the simplicity of the procedure for LDG gradient separation measurement, compared with immunofluorescence analysis, which requires an expensive fluorescent microscope, LDGs may be more clinically useful than NETs, particularly in resource-limited settings. Although LDGs cannot differentiate between less severe and severe COVID-19, unlike NETs assessed by DAPI, initial evaluation by chest radiography plus LDGs may be an economically viable predictor of the need for IMV. Furthermore, detection of NETs in the LDG fraction may be another parameter reflecting COVID-19 severity, as NETs percentage in LDGs appears to be elevated in patients with more severe COVID-19 infection and CKD stage 5D. More studies to explore clinical use of LDGs are warranted.

Acknowledgments

W.C., S.K., W.A., H.H., O.T., A.L., M.J.S., and C.R. conceptualized and supervised the study and wrote the manuscript; W.C., S.K., and A.L. provided data and data analysis; W.C., T.B., and A.L. performed statistical analysis; all authors except H.H., M.J.S., and C.R. provided clinical care for the patients described; W.C. obtained funding; all authors edited and approved the final version of the paper; and W.C., S.K., O.T., A.L., M.J.S., and C.R. provided overall direction for the project and responsible for the final version of the manuscript.

Disclosure statement

No potential conflict of interest was reported by the author(s).

Funding

This research project is supported by Mahidol University (Fundamental Fund; Basic Research Fund: fiscal year 2022).

Data availability statement

The datasets used and/or analyzed during the current study are available from the corresponding authors on reasonable request.

References

[1] Saithong S, Worasilchai N, Saisorn W, et al. Neutrophil extracellular traps in severe SARS-CoV-2 infection: a possible impact of LPS and (1→3)-β-D-glucan in blood from gut translocation. Cells. 2022;11(7):1103. doi: 10.3390/cells11071103.
[2] Looi M-K. How are covid-19 symptoms changing? BMJ. 2023;380p :3. doi: 10.1136/bmj.p3.
[3] Li J, Ghosh TS, McCann R, et al. Robust cross-cohort gut microbiome associations with COVID-19 severity. Gut Microbes. 2023;15(1):2242615. doi: 10.1080/19490976.2023.2242615.
[4] Chenchula S, Vidyasagar K, Pathan S, et al. Global prevalence and effect of comorbidities and smoking status on severity and mortality of COVID-19 in association with age and gender: a systematic review, meta-analysis and meta-regression. Sci Rep. 2023;13(1):6415. doi: 10.1038/s41598-023-33314-9.
[5] Cancarevic I, Nassar M, Daoud A, et al. Mortality rate of COVID-19 infection in end stage kidney disease patients on maintenance hemodialysis: a systematic review and meta-analysis. World J Virol. 2022;11(5):352–361. doi: 10.5501/wjv.v11.i5.352.
[6] Gur E, Levy D, Topaz G, et al. Disease severity and renal outcomes of patients with chronic kidney disease infected with COVID-19. Clin Exp Nephrol. 2022;26(5):445–452. doi: 10.1007/s10157-022-02180-6.
[7] Chancharoenthana W, Kamolratanakul S, Visitchanakun P, et al. Lacticaseibacilli attenuated fecal dysbiosis and metabolome changes in Candida-administered bilateral nephrectomy mice. Front Immunol. 2023;14:1131447. doi: 10.3389/fimmu.2023.1131447.

[8] Tungsanga S, Katavetin P, Panpetch W, et al. Lactobacillus rhamnosus L34 attenuates chronic kidney disease progression in a 5/6 nephrectomy mouse model through the excretion of anti-inflammatory molecules. Nephrol Dial Transplant. 2022;37(8):1429–1442. doi: 10.1093/ndt/gfac032.
[9] Issara-Amphorn J, Dang CP, Saisorn W, et al. Candida administration in bilateral nephrectomy mice elevates serum (1→3)-β-D-glucan that enhances systemic inflammation through energy augmentation in macrophages. Int J Mol Sci. 2021;22(9):5031.
[10] Chancharoenthana W, Kamolratanakul S, Leelahavanichkul A, et al. Gastrointestinal manifestations of long-term effects after COVID-19 infection in patients with dialysis or kidney transplantation: an observational cohort study. World J Gastroenterol. 2023;29(19):3013–3026. doi: 10.3748/wjg.v29.i19.3013.
[11] Mahoney R, Lee GK, Zepeda JP, et al. Severe manifestations and treatment of COVID-19 in a transplanted patient with Fabry disease. Mol Genet Metab Rep. 2021;29:100802. doi: 10.1016/j.ymgmr.2021.100802.
[12] Sae-Khow K, Charoensappakit A, Chiewchengchol D, et al. High-dose intravenous ascorbate in sepsis, a pro-oxidant enhanced microbicidal activity and the effect on neutrophil functions. Biomedicines. 2022;11(1):51. doi: 10.3390/biomedicines11010051.
[13] Saisorn W, Saithong S, Phuengmaung P, et al. Acute kidney injury induced lupus exacerbation through the enhanced neutrophil extracellular traps (and apoptosis) in Fcgr2b deficient lupus mice with renal ischemia reperfusion injury. Front Immunol. 2021;12:669162. doi: 10.3389/fimmu.2021.669162.
[14] Saithong S, Saisorn W, Dang CP, et al. Candida administration worsens neutrophil extracellular traps in renal ischemia reperfusion injury mice: an impact of gut fungi on acute kidney injury. J Innate Immun. 2022;14(5):502–517. doi: 10.1159/000521633.
[15] Ning X, Wang WM, Jin HZ. Low-density granulocytes in immune-mediated inflammatory diseases. J Immunol Res. 2022;2022:1622160–11. doi: 10.1155/2022/1622160.
[16] Dean LS, Devendra G, Jiyarom B, et al. Phenotypic alteration of low-density granulocytes in people with pulmonary post-acute sequalae of SARS-CoV-2 infection. Front Immunol. 2022;13:1076724. doi: 10.3389/fimmu.2022.1076724.
[17] Rodríguez-Carrio J, Carrillo-López N, Ulloa C, et al. A subset of low density granulocytes is associated with vascular calcification in chronic kidney disease patients. Sci Rep. 2019;9(1):13230. doi: 10.1038/s41598-019-49429-x.
[18] Saithong S, Saisorn W, Visitchanakun P, et al. A synergy between endotoxin and (1→3)-beta-D-glucan enhanced neutrophil extracellular traps in Candida administered dextran sulfate solution induced colitis in FcGRIIB−/− lupus mice, an impact of intestinal fungi in lupus. J Inflamm Res. 2021;14:2333–2352. doi: 10.2147/JIR.S305225.
[19] Liana P, Liberty IA, Murti K, et al. A systematic review on neutrophil extracellular traps and its prognostication role in COVID-19 patients. Immunol Res. 2022;70(4):449–460. doi: 10.1007/s12026-022-09293-w.
[20] Caudrillier A, Kessenbrock K, Gilliss BM, et al. Platelets induce neutrophil extracellular traps in transfusion-related acute lung injury. J Clin Invest. 2012;122(7):2661–2671. doi: 10.1172/JCI61303.
[21] Shang Y, Liu T, Wei Y, et al. Scoring systems for predicting mortality for severe patients with COVID-19. EClinicalMedicine. 2020;24:100426. doi: 10.1016/j.eclinm.2020.100426.
[22] Chan WY, Hamid MTR, Gowdh NFM, et al. Chest radiograph (CXR) manifestations of the novel coronavirus disease 2019 (COVID-19): a mini-review. Curr Med Imaging. 2021;17(6):677–685. doi: 10.2174/1573405616666201231103312.
[23] Chancharoenthana W, Wattanatorn S, Vadcharavivad S, et al. Agreement and precision analyses of various estimated glomerular filtration rate formulae in cancer patients. Sci Rep. 2019;9(1):19356. doi: 10.1038/s41598-019-55833-0.
[24] Mummery RS, Rider CC. Characterization of the heparin-binding properties of IL-6. J Immunol. 2000;165(10):5671–5679. doi: 10.4049/jimmunol.165.10.5671.
[25] Zhou F, Yu T, Du R, et al. Clinical course and risk factors for mortality of adult inpatients with COVID-19 in Wuhan, China: a retrospective cohort study. Lancet. 2020;395(10229):1054–1062. doi: 10.1016/S0140-6736(20)30566-3.
[26] Atallah B, Mallah SI, AlMahmeed W. Anticoagulation in COVID-19. Eur Heart J Cardiovasc Pharmacother. 2020;6(4):260–261. doi: 10.1093/ehjcvp/pvaa036.
[27] Makjaroen J, Thim-Uam A, Dang CP, et al. A comparison between 1 day versus 7 days of sepsis in mice with the experiments on LPS-activated macrophages support the use of intravenous immunoglobulin for sepsis attenuation. J Inflamm Res. 2021;14:7243–7263. doi: 10.2147/JIR.S338383.
[28] Moslehi N, Jahromy MH, Ashrafi P, et al. Multi-organ system involvement in coronavirus disease 2019 (COVID-19): a mega review. J Family Med Prim Care. 2022;11(9):5014–5023. doi: 10.4103/jfmpc.jfmpc_1570_21.
[29] Amornphimoltham P, Yuen PST, Star RA, et al. Gut leakage of fungal-derived inflammatory mediators: part of a gut-liver-kidney axis in bacterial sepsis. Dig Dis Sci. 2019;64(9):2416–2428. doi: 10.1007/s10620-019-05581-y.
[30] Lara-Prado JI, Pazos-Pérez F, Méndez-Landa CE, et al. Acute kidney injury and organ dysfunction: what is the role of uremic toxins? Toxins. 2021;13(8):551. doi: 10.3390/toxins13080551.
[31] Dela Cruz PTH, Davison D, Yamane DP, et al. Increased endotoxin activity in COVID-19 patients admitted to the intensive care unit. J Intensive Care Med. 2023;38(1):27–31. doi: 10.1177/08850666221121734.
[32] Khan S, Bolotova O, Sahib H, et al. Endotoxemia in critically ill patients with COVID-19. Blood Purif. 2022;51(6):513–519. doi: 10.1159/000518230.

[33] Tungsanga S, Panpetch W, Bhunyakarnjanarat T, et al. Uremia-induced gut barrier defect in 5/6 nephrectomized mice is worsened by candida administration through a synergy of uremic toxin, lipopolysaccharide, and (1→3)-β-D-glucan, but is attenuated by *Lacticaseibacillus rhamnosus* L34. Int J Mol Sci. 2022;23(5):2511. doi: 10.3390/ijms23052511.
[34] Lemesch S, Ribitsch W, Schilcher G, et al. Mode of renal replacement therapy determines endotoxemia and neutrophil dysfunction in chronic kidney disease. Sci Rep. 2016;6(1):34534. doi: 10.1038/srep34534.
[35] Lotfi R, Kalmarzi RN, Roghani SA. A review on the immune responses against novel emerging coronavirus (SARS-CoV-2). Immunol Res. 2021;69(3):213–224. doi: 10.1007/s12026-021-09198-0.
[36] Pieniazek A, Bernasinska-Slomczewska J, Gwozdzinski L. Uremic toxins and their relation with oxidative stress induced in patients with CKD. Int J Mol Sci. 2021;22(12):6196.
[37] Bello S, Lasierra AB, López-Vergara L, et al. IL-6 and cfDNA monitoring throughout COVID-19 hospitalization are accurate markers of its outcomes. Respir Res. 2023;24(1):125. doi: 10.1186/s12931-023-02426-1.
[38] Celec P, Vlková B, Lauková L, et al. Cell-free DNA: the role in pathophysiology and as a biomarker in kidney diseases. Expert Rev Mol Med. 2018;20:e1. doi: 10.1017/erm.2017.12.
[39] Siavoshi F, Safavi-Naini SAA, Shirzadeh Barough S, et al. On-admission and dynamic trend of laboratory profiles as prognostic biomarkers in COVID-19 inpatients. Sci Rep. 2023;13(1):6993. doi: 10.1038/s41598-023-34166-z.
[40] Wu J, Cyr A, Gruen DS, et al. Lipidomic signatures align with inflammatory patterns and outcomes in critical illness. Nat Commun. 2022;13(1):6789. doi: 10.1038/s41467-022-34420-4.
[41] Menez S, Moledina DG, Thiessen-Philbrook H, et al. Prognostic significance of urinary biomarkers in patients hospitalized with COVID-19. Am J Kidney Dis. 2022;79(2):257–267.e1. doi: 10.1053/j.ajkd.2021.09.008.
[42] Gómez-Pastora J, Weigand M, Kim J, et al. Hyperferritinemia in critically ill COVID-19 patients - Is ferritin the product of inflammation or a pathogenic mediator? Clin Chim Acta. 2020;509:249–251. doi: 10.1016/j.cca.2020.06.033.
[43] Kim JK, Hong CW, Park MJ, et al. Increased neutrophil extracellular trap formation in uremia is associated with chronic inflammation and prevalent coronary artery disease. J Immunol Res. 2017;2017:8415179–10. doi: 10.1155/2017/8415179.
[44] Kim JK, Park MJ, Lee HW, et al. The relationship between autophagy, increased neutrophil extracellular traps formation and endothelial dysfunction in chronic kidney disease. Clin Immunol. 2018;197:189–197. doi: 10.1016/j.clim.2018.10.003.
[45] Talal S, Mona K, Karem A, et al. Neutrophil degranulation and severely impaired extracellular trap formation at the basis of susceptibility to infections of hemodialysis patients. BMC Med. 2022;20(1):364. doi: 10.1186/s12916-022-02564-1.
[46] Chancharoenthana W, Tiranathanagul K, Srisawat N, et al. Enhanced vascular endothelial growth factor and inflammatory cytokine removal with online hemodiafiltration over high-flux hemodialysis in sepsis-related acute kidney injury patients. Ther Apher Dial. 2013;17(5):557–563. doi: 10.1111/1744-9987.12016.
[47] Piotte J, Louis F, Buyansky D, et al. Online hemodiafiltration compared to conventional hemodialysis in critically ill patients. Kidney Int Rep. 2022;7(11):2376–2387. doi: 10.1016/j.ekir.2022.08.007.
[48] Wildhagen KC, García de Frutos P, Reutelingsperger CP, et al. Nonanticoagulant heparin prevents histone-mediated cytotoxicity in vitro and improves survival in sepsis. Blood. 2014;123(7):1098–1101. doi: 10.1182/blood-2013-07-514984.
[49] Lam FW, Cruz MA, Parikh K, et al. Histones stimulate von Willebrand factor release in vitro and in vivo. Haematologica. 2016;101(7):e277-9–e279. doi: 10.3324/haematol.2015.140632.
[50] McGrath RT, McRae E, Smith OP, et al. Platelet von Willebrand factor–structure, function and biological importance. Br J Haematol. 2010;148(6):834–843. doi: 10.1111/j.1365-2141.2009.08052.x.
[51] van der Vorm LN, Visser R, Huskens D, et al. Circulating active von Willebrand factor levels are increased in chronic kidney disease and end-stage renal disease. Clin Kidney J. 2020;13(1):72–74. doi: 10.1093/ckj/sfz076.
[52] Ngo AT, Skidmore A, Oberg J, et al. Platelet factor 4 limits neutrophil extracellular trap- and cell-free DNA-induced thrombogenicity and endothelial injury. JCI Insight. 2023;8(22):e171054. doi: 10.1172/jci.insight.171054.